Spatial Resolution in Vector Potential Photo-electron Microscopy

Raymond Browning

VPPEM uses the magnetic vector potential field as a spatially resolved reference for image formation. A magnet with a uniform field region, such as a solenoid, is used to create a cylindrically symmetric vector potential field which acts as a two dimensional reference. The sample to be imaged is immersed in the center of the field, and illuminated by a UV or X-ray photon beam. The resultant photoelectrons are emitted into the vector potential field, and travel down magnetic field lines in cyclotron orbits towards a ferromagnetic shield with an aperture. When the photoelectrons leave the vector potential field by passing through the aperture in the ferromagnetic shield, they gain off-axis momentum in the radial, and azimuthal directions that depends on their position in the vector potential field at the sample. The momentum distribution gained from the sudden change in the vector potential field at the aperture forms an angular image of the electron emission. The vector potential field is a momentum field with dimensions of momentum per unit charge. When an electron leaves the field suddenly, it gains momentum due to its charge:

$$\mathbf{p} = -e\mathbf{A} \qquad (1)$$

Where e is the charge on the electron, $\mathbf{A}$ is the vector potential at the aperture, and the off-axis momentum is **p**. The off-axis gain in momentum creates the angular image. The photoelectrons have chemical information from the sample in the electron energy spectrum, and two dimensional spatial information from the magnetic vector potential field. The resulting angular electron image can be passed through an electron energy analyzer to produce a photoelectron spectroscopic (PES) image.

We can illustrate the mechanics of VPPEM image formation with a simulation of the exit of electron trajectories from a simple magnetic circuit.

Fig. 1 shows a magnet set in a soft iron yoke with a tapered aperture for the exit of electrons from the field. The magnetic axis is rotationally symmetric around the horizontal axis. The volume near the magnet face has a constant magnetic field, and therefore the vector potential field is a radially increasing circular vector field.

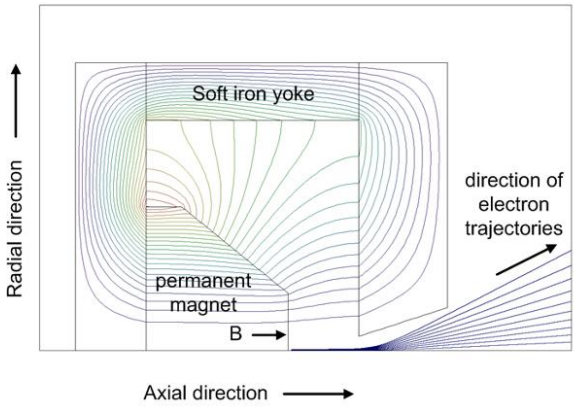

Fig. 1 Electron trajectories in a magnetic circuit composed of a permanent magnet in a ferromagnetic yoke with a tapered aperture

Fig. 1 shows a set of electron trajectories which begin at equally spaced radial points just off the axis near the pole piece. The electron trajectories initially travel along parallel to the optical axis, and are constrained into a narrow beam by the magnetic field lines near the axis. There is a small magnification of the radial distances as the magnetic field weakens moving away from the pole piece. When the electrons exit the field through the aperture, they leave the field lines, and become deflected away from the axis by the change in the vector potential. The deflection produces an angular distribution dependent on the initial radial distribution in the vector potential field.

Only the radial distances are plotted in Fig. 1, the electron trajectories are rotated out of the plane of the diagram. The deflection angles agree with Equation 1 to a few percent, and are slightly dependent on the details of the aperture. The simulation shows the deflection angles are proportional to the radial positions at the origin for small, and moderate angles.

If the electron trajectories are emitted at to an angle to the magnetic axis they follow cyclotron orbits until they exit the aperture where they are deflected into a final direction. This is illustrated in Fig. 2.

Fig. 2 shows a simulated trajectory of a 500eV electron from a 1T field emitted at 45^{o} to the magnetic axis, and at a small distance off-axis in the x direction. In Fig. 2 we are looking down the magnetic axis. We see the cyclotron orbit move away from the y axis, and expand as the field decreases. As the trajectory exits the field, it undergoes a deflection into its final direction. Clearly, the final direction will depend on exactly where the orbit crosses the aperture as the vector potential varies across the

aperture. If we simulate multiple starting points along the axis, the direction changes with the off-axis trajectories forming an angular cone.

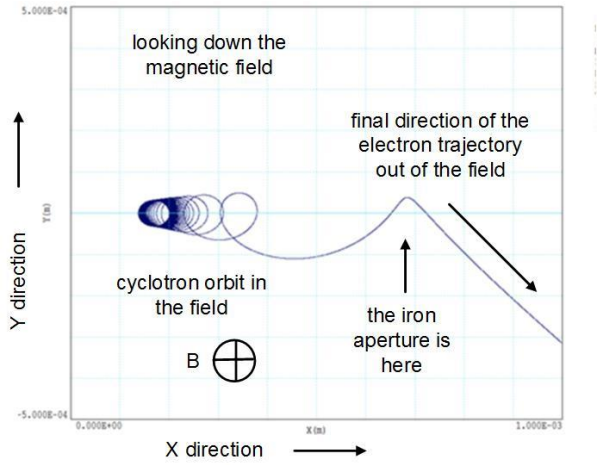

Fig. 2 An electron orbit in the magnetic circuit of Fig. 1 looking down the magnetic axis

If we start the simulation of Fig. 2 with a range of off axis angles from 0° to 90°, and with a weighting for a cosine emission distribution, if there are no other off-axis effects, we would expect to get a cone of confusion equivalent to the disk of confusion from a magnetic projection microscope. This is what we find. By ray tracing over the full range of angles, we can see the VPPEM cone of confusion is simply caused by the variation of the exit point in the vector potential field at the aperture.

In the VPPEM, electrons of all energies from a sample are deflected into an angular image by the change in vector potential at the aperture. The angular image can be converted into a monochromatic real image focused at an image plane.

We can calculate the point spread function (PSF) by considering the possible contributions to the electron off-axis momentum. These contributions are from the angular momentum of the cyclotron orbit, and the vector potential.

As an electron leaves the field line, it retains angular momentum **L** from the cyclotron orbit.

$$\mathbf{L} = \mathbf{r} \times m\mathbf{v} \qquad (2)$$

Where **r** is the orbit radius, m the electron mass, and **v** the orbital velocity. As the cyclotron orbit unwinds to an infinite radius conservation of angular momentum implies that the off-axis momentum due to the velocity of the electrons in the obit must go to zero. Using a full simulation of the electron orbits, the off-axis motion due to the orbital velocity at the aperture can be shown to go to zero. Although it is difficult to observe in a trajectory such shown in Fig 2. Then the only contribution to the off-axis momentum in the image is the vector potential at the aperture. Note: because the distance across the cyclotron orbit is the same as that at a magnetic projection microscope detector, the disk of confusion has the same form as in the magnetic projection microscope, but translated into an angular disk of confusion.

The disk of confusion is created by electrons being emitted at all angles up to 90° from the magnetic axis. The maximum off-axis distance is twice the maximum radius. The helical trajectories have a maximum radius that depend on the energy of the electrons *E*, and the magnetic field *B*, in the following relationship[2]:

$$r_{\max} = \frac{\sqrt{2mE}}{eB} \qquad (3)$$

The probability of being at a distance *x* from the point of emission can be calculated using the geometry of Fig. 3.

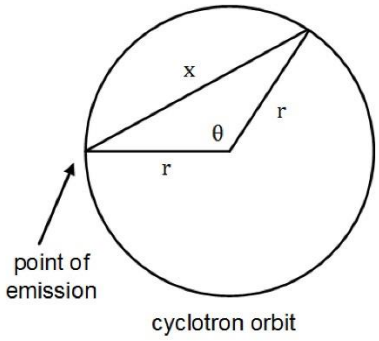

Fig. 3 Construction to calculate the VPPEM PSF

The cyclotron orbit is illustrated by the circle of radius *r*. The point the electron crosses the image plane will be a distance *x* from the point of emission where *x* is given by the cosine law:

$$x^2 = 2r^2 - 2r^2\cos(\theta) \qquad (4)$$

$$\theta = \cos^{-1}\left(1 - \frac{x^2}{2r^2}\right) \qquad (5)$$

During one cyclotron cycle, the probability of being between *x* and *x+dx* will depend on the time, Δ*t*, spent in the interval *dx* over the cycle. If the cycle time is *T*, and the velocity in x is *dx/dt* then, as time is distance/velocity we have the probability *P(x):*

$$P(x) = \frac{\Delta t}{T} = \frac{1}{T}\frac{dt}{dx}dx = \frac{1}{T}\frac{dt}{d\theta}\frac{d\theta}{dx}dx \quad (6)$$

The angular speed is constant:

$$\frac{d\theta}{dt} = \frac{2\pi}{T} \quad (7)$$

Differentiating Equation 5 to find $d\theta / dx$, and substituting with Equation 7 into Equation 6 the probability of an electron crossing the image plane between x and $x + dx$ is:

$$P(x) = \frac{1}{2\pi\left(1 - \frac{x^2}{4r^2}\right)^{1/2}}dx \quad (8)$$

Equation 8 is for a single radius *r*. The single electron radius must be convolved with distribution of emitted radii which we assume is a cosine distribution. This gives the one dimensional PSF. Dividing the result by 2πr, the area of the PSF at a radius *r*, gives the cross section of the two dimensional PSF as shown in Fig. 5.

While the two dimensional PSF is sharply peaked at the center, nearly 50% of the integrated intensity is at a radius greater than 1.0 r_{max}.

The spatial resolution is determined by the energy of the electrons at the sample, and the strength of the vector field. We can convolve the PSF of Fig. 5 with a step function to simulate the edge response. A good approximation of the edge resolution defined as the 20% to 80% change is $3\sqrt{E}/B$ microns with E in electron volts, and B in Tesla. Electrons emitted with 1eV energy in a 2T field can be imaged with an edge resolution of 1.5 microns.

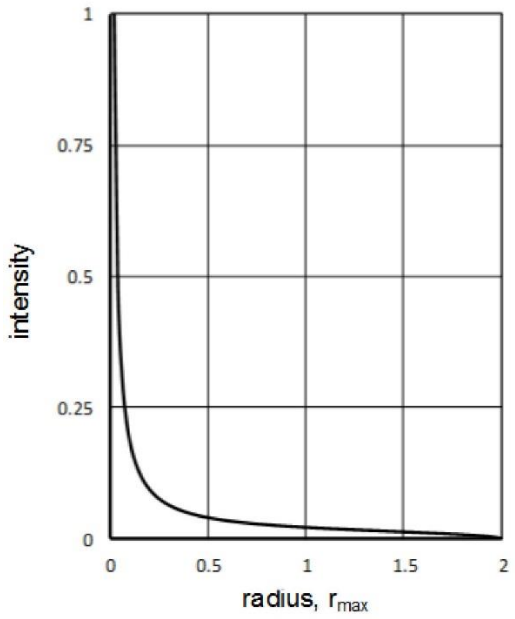

Fig. 5 Two dimensional PSF for a VPPEM in units of the maximum cyclotron radius

The energy of the electrons can be changed along the trajectories within the field by biasing the sample. This change of energy does not change the spatial resolution which is determined solely by the electron emission energy. The angle of deflection is inversely proportional to the square root of the energy of the electrons when they exit the field. However, the angles of the cyclotron orbits also change in the same way as the electrons are accelerated or decelerated.

This means that in the VPPEM we can change the electron energy that we image from the sample without having to change the energy of the electrons exiting the vector potential field. This implies that the magnification of the system is the same for all energies, and comparing the spatial resolution at different emission energies is straightforward.

Using a fixed photon energy of 80eV, and scanning across the edge of a cleaved Si wafer to measure the 20-80% edge resolution for different emitted electron energies gives us the results shown in Fig 5.

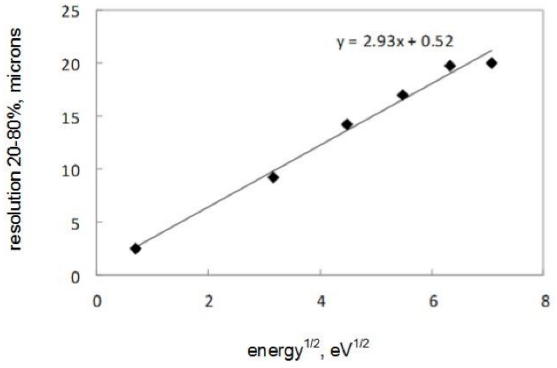

Fig. 6 Experimental measurement of the 20-80% edge resolution for electron emission energies between 0.5eV and 50eV

Fig. 6 shows the resolution measured across the cleaved Si wafer edge for different energies from 0.5eV to 50eV, and a field at the sample of 1 Tesla. The energy resolution is 0.25eV, and the length scale was established using a 600 mesh Au grid. The plot is of the 20-80% edge resolution verses the square root of the electron energy at the sample in electron volts. The slope of the plot is 2.93 very close to the simulated estimate.

In conclusion a good approximation for edge resolution of the VPPEM is $3\sqrt{E}/B$ in microns with E in electron volts and B in Tesla.

References

[1]R.Browning Rev. Sci. Instrum. **82**, 103703 (2011)

[2]G. Beamson, Q. Porter, and D. W. Turner J. Phys. E: Scient. Instrum. **13** 64-66 (1980)

[3]G. Beamson, Q. Porter, and D. W. Turner, Nature **290**, 556 (1981).

[4]P. Kruit, and F. H. Reed, J. Phys. E **16**, 313 (1983).